

Pore pressure response of seabed in standing waves and its mechanism



Hu Wang^a, Hong-jun Liu^{a,b,*}, Min-sheng Zhang^{a,b}

^a Key Laboratory of Marine Environment & Ecology, Ministry of Education, Qingdao 266100, China

^b College of Environmental Science and Engineering, Ocean University of China, Qingdao 266100, China

ARTICLE INFO

Article history:

Received 3 July 2013

Received in revised form 11 June 2014

Accepted 13 June 2014

Available online xxxx

Keywords:

Standing waves

Silt

Excess pore pressure

Volumetric strain

Theoretical model

ABSTRACT

Experiments were carried out in a newly-developed rectangular flume to investigate the pore pressure response of silty seabed in standing waves, and to emphatically discuss the physical mechanism of wave-induced pore pressure. We first analyzed the features of wave-induced stress, laid out the experimental setup, and particularly monitored the temporal and spatial variation of pore pressure. Then, we summarized the physical essence of wave-induced pore pressure, discussed the applicability of the existing models, and proposed several key points about developing new models. Results indicate that regular standing waves were obtained in the rectangular flume. The oscillating pore pressure (OPP) and the residual pore pressure (RPP) were observed simultaneously in the seabed under wave nodes or antinodes, and were found with coupling effect. The OPP and RPP were related to the elastic and plastic volumetric strains, respectively. Both elastic and plastic volumetric strains may be caused by the wave-induced cyclic spherical stress or deviatoric stress. The elastic model could only simulate the OPP and the pore pressure development mode could only simulate the RPP. The yielding under isotropic compression and the shear expansion of geotechnical materials, as well as the wave-induced stress paths, should be considered in the elastoplastic model to simulate the wave-induced pore pressure accurately.

© 2014 Elsevier B.V. All rights reserved.

1. Introduction

The wave-induced instability of seabed foundation always threatens the security and normal use of offshore structures such as breakwaters, platforms, wind turbines and pipelines. Considerable experimental and theoretical works have been done recently, including the response of single seabed under wave loads (Chang et al., 2007; Chowdhury et al., 2006; Clukey et al., 1985; Foda and Tzang, 1994; Hsu and Jeng, 1994; Jeng et al., 2010; Kirca et al., 2013; Miyamoto et al., 2004; Sassa and Sekiguchi, 1999; Sumer et al., 2006; Tzang and Ou, 2006; Yamamoto et al., 1978), and the coupled response of structure and seabed due to wave loads (De Groot et al., 2006a, 2006b; Jeng et al., 2013; Li and Jeng, 2008; Sumer et al., 1999; Sumer et al., 2007; Teh et al., 2003; Zhou et al., 2011).

The wave-induced seabed instability can be classified into three modes: liquefaction, shear failure and scour (Jeng, 2003; Sumer and Fredsøe, 2002), which may occur separately or simultaneously. Nevertheless, the wave-induced pore pressure, especially the excess pore pressure (EPP), is particularly important for any modes. Liquefaction may occur in an extreme case when EPP is equal to the effective self weight of the overburden (e.g. Zen and Yamazaki, 1990). The risk of shear failure may be promoted since the effective shear strength of the

seabed soil can be significantly reduced by EPP (e.g. Zen et al., 1998). The EPP induced upward seepage force may promote the suspension and scour of the seabed soil (e.g. Tzang et al., 2009). Thus, figuring out the distribution and variation of wave-induced EPP in the seabed is very important and necessary for coastal engineers.

The wave-induced EPP in the seabed can be divided into two parts: transient or OPP which fluctuates around an equilibrium position periodically, and accumulative or RPP which continuously builds up with continuous wave loads (Jeng, 2003; Sumer and Fredsøe, 2002). In the past few decades, numerous experiments and theoretical models were developed to study the wave-induced EPP. However, more work is still needed, particularly on the pore pressure response of silty seabed in standing waves, and the physical mechanism between experimental phenomena and theoretical models. In this paper, we investigated the pore pressure response of silty seabed in standing waves with a newly-developed rectangular wave flume, through which we hope to enrich experimental methods and data. Based on the experimental results and the existing findings in literatures, we discussed the physical mechanism of wave-induced pore pressure to make a better understanding of the theoretical models.

2. Experiments

2.1. Wave-induced stress in the seabed

In the real ocean environment, a complex wave can be regarded as a superposition of simple waves, such as sinusoidal wave. EPP is essentially

* Corresponding author at: Key Laboratory of Marine Environment & Ecology, Ministry of Education, No. 238, Songling Road, Laoshan District, Qingdao 266100, China. Tel./fax: +86 0532 66782573.

E-mail address: hongjun@ouc.edu.cn (H. Liu).

caused by the wave-induced stress which has changed the original stress field in the seabed. The feature points of the wave profile include antinodes (crests and troughs) and nodes. With sinusoidal wave for example, the wave-induced stress of the soil elements in the seabed under different wave phases is shown in Fig. 1. With the propagation of wave, a fixed soil element under the feature points experiences periodical change of 1–2–3–4–1 (Fig. 1). The permeability of the seabed soil changes from 10^{-3} to 10^{-6} m/s for sands and silts, which is pretty small during each wave cycle in seconds and can be ignored. Thus, the seabed surface is supposed to be undrained, and the wave-induced dynamic pressure P can be applied on the seabed surface as a total stress. Based on the linear wave theory, P is given as:

$$P = \frac{\gamma_w H}{2 \cosh(kh)} \sin(kx - \omega t) \quad (1)$$

where γ_w is the unit weight of sea water, H is the wave height, k is the wave number, h is the water depth, ω is the angular frequency, x is the horizontal ordinate and t is time.

With the still water level as reference, the maximum water depth appears at the wave crest and Element 1 endures the maximum vertical compressive stress σ'_{\max} . The minimum vertical compressive stress σ'_{\min} acts on Element 3 when the minimum water depth appears at the wave trough, as shown in Fig. 1. Clearly, the two types of wave-induced stresses are equal in magnitude but opposite in direction. The water level does not change any more at wave nodes, indicating that there is no vertical compressive stress but maximum horizontal shear stress acting on Elements 2 and 4. The wave-induced stress path of a soil element in the seabed due to progressive sinusoidal wave is shown in Fig. 2a. The amplitude of wave-induced stress is constant, but the direction overturns within half a wave cycle. The rotation of principal stress of wave loads is also remarkably different from other loads (Ishihara and Towhata, 1983; Shen et al., 1994). If the cyclic vertical compressive stress is considered alone, based on the stress path shown in Fig. 2b, only spherical stress changes and thus only transient pore pressure will occur according to Zen and Yamazaki (1990). The residual mechanism works when only the cyclic deviatoric stress is considered (Seed and Rahman, 1978) according to the stress path in Fig. 2c. Interestingly, Fig. 2b and c just shows the stress paths of soil element under antinodes and nodes of standing wave, respectively. Actually, the stress conditions of the soil element in the seabed are changing periodically, while the vertical compression alternates with the horizontal shear (Fig. 2a). However, the two types of wave-induced stress can be separated under antinodes and nodes. Therefore, we can explore the contributions to OPP and RPP due to the two types of

wave-induced stresses in standing waves. Next, we designed a rectangular flume to generate standing waves, and carried out a series of experiments.

2.2. Experimental setup and design

The experiment was conducted in a rectangular flume dimensioned with 120 cm long, 60 cm wide and 120 cm high (Fig. 3). A wave-making system was designed with a motor-driven cylindrical oscillator slightly less than 60 cm wide. The system was equipped in the middle of the flume's length direction. A symmetric reflective standing wave was generated by adjusting the motor's speed, and the oscillator's diameter and sinking depth into water. The process of wave generation is illustrated in Fig. 4: When the oscillator went downwards, wave was generated and propagated towards the two sides (Fig. 4a); Waves reflected when they reached the side wall (Fig. 4b); Reflected waves and oscillator-generated waves were in superposition (Fig. 4c). Standing waves with constant height were generated after several cycles of reflection and superposition. The antinodes were located at the middle and the two sides of the flume's length direction, while the nodes appeared at the two quarters. Corresponding to Fig. 1, the antinodes only experienced the change of crest-trough-crest, and the soil element below only experienced cyclic spherical stress (Fig. 2b). The water level did not change any more at the nodes, and therefore, the soil element only experienced cyclic deviatoric stress (Fig. 2c). Pore pressure transducers were equipped at the vertical profiles in the seabed soil under the nodes and antinodes separately so as to identify perfect experimental sites for studying the mechanism of wave-induced EPP. In addition, the rectangular flume system is smaller and cheaper than the traditional wave flume used by Sumer et al. (2006) and Tzang and Ou (2006).

The soil mainly composed of feldspar and quartz was collected from the tidal flat of the Yellow River delta. It is a typical silt with specific gravity $G_s = 2.71$, plasticity index $I_p = 9.4$ and median size $d_{50} = 0.041$ mm. The soil samples were dried, crushed, mixed with water and stirred well into mud. Test series with a piezoresistive pore pressure transducer ($\phi 20 \times 53$ mm, full range 5 psi, accuracy 0.2%, Nanjing Hydraulic Research Institute, China) were conducted before the mud was placed into the flume. The test series were placed at three profiles (Fig. 3a): Profile 1-1 near the seabed surface monitors the dynamic pressure at seabed surface; Profile 2-1 and Profile 3-1 under antinodes and nodes, respectively, measure the pore pressure in the seabed. The transducers were deployed on a tripod stand to avoid displacement during wave cycles, and the stand was placed in the middle across the flume's width to reduce possible side effects. The pore pressure signals were acquired by a DAQLab2005 acquisition system (Iotech, Cleveland,

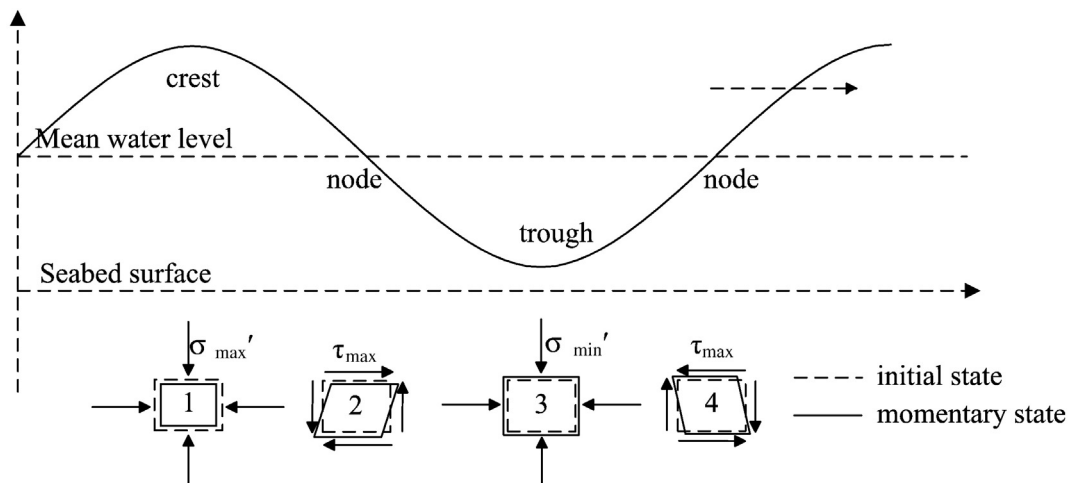


Fig. 1. Wave-induced stress in seabed.

Download English Version:

<https://daneshyari.com/en/article/8059826>

Download Persian Version:

<https://daneshyari.com/article/8059826>

[Daneshyari.com](https://daneshyari.com)